A Microfluidic Device with Continuous Ligand Gradients in Supported Lipid Bilayers to Probe Effects of Ligand Surface Density and Solution Shear Stress on Pathogen Adhesion

Jasper van Weerd, Shrikrishnan Sankaran, Oliver Roling, Sertan Sukas, Sven Krabbenborg, Jurriaan Huskens, Séverine le Gac, Bart Jan Ravoo, Marcel Karperien, and Pascal Jonkheijm**

Studying binding interactions involving living cells requires a platform that carefully mimics the physiological parameters that govern these phenomena. Very often the amount of ligands that receptors can bind affect overall binding strength as is the case in cell adhesion. In addition, the physical environment can strongly influence these processes. This is exemplified by the effect of shear stress in catch-bond-mediated binding of bacteria. Traditional analysis techniques do not allow to probe these factors simultaneously. To this end, continuous ligand gradients in locked-in supported lipid bilayers (SLBs) are prepared in a microfluidic device to control fluid flow. This platform allows for one-pot characterization of cell surface binding events and 1) the effect of ligand density and 2) shear stress, simultaneously. The model interaction between the FimH receptor found on *Escherichia coli* and mannose found on the mammalian cell membrane is used to evaluate the platform. Using a single chip, specific *E. coli* ORN 178 adhesion (K_d of 0.9×10^{-21} M), detachment and displacement are shown to depend on the mannose-density and shear stress. For the first time, these effects are studied in a single chip device with high quality. This chip provides entry to further our understanding of other cell–cell interactions.

1. Introduction

Living cells are constantly exposed to a variety of external chemical stimuli, such as hormones, growth factors, and virulence factors, which are received either in soluble form from extracellular fluids, or through direct cell–cell contacts.[1] Cell-surface receptors can interact with molecular signals on opposing cells via specific binding to ligand molecules. In nature, biochemical mechanisms exist to translate that binding into a cellular response.[2] In this way, intercellular interactions can be as diverse as the binding of pathogens to their target tissues, sperm-egg binding, interactions among cells in the immune system, and recognition among cells during embryonic development.[3] Numerous techniques have been developed to improve our understanding of the molecular basis of cell–cell recognition and have consequently made significant implications for improved intervention in many areas of biology and medicine.[3a,4] For example, glycan arrays have been extremely successful in determining the binding characteristics of pathogens toward carbohydrates that are usually found on target cell surfaces. However, determining the effect of glycan surface density has been proven to be more demanding to analyze.[5] Usually strategies require the preparation of several arrays or surfaces with discrete ligand densities, a cumbersome process prone to inaccuracies while the information is biased by the preselected ligand concentrations.[5a–c]

Dr. J. van Weerd, S. Sankaran, Prof. P. Jonkheijm
Bioinspired Molecular Engineering Laboratory
University of Twente
MIRA Institute for Biomedical Technology and Technical Medicine
P.O. Box 217, 7500 AE, Enschede, Netherlands
E-mail: p.jonkheijm@utwente.nl

Dr. J. van Weerd, Prof. M. Karperien
Department of Developmental BioEngineering
University of Twente
MIRA Institute for Biomedical Technology and Technical Medicine
P.O. Box 217, 7500 AE, Enschede, Netherlands
E-mail: h.b.j.karperien@utwente.nl

DOI: 10.1002/admi.201600055

Dr. J. van Weerd, S. Sankaran, Dr. S. O. Krabbenborg, Prof. J. Huskens, Prof. P. Jonkheijm
Molecular nanoFabrication group
University of Twente
MESA+ Institute for Nanotechnology
P.O. Box 217, 7500 AE, Enschede, Netherlands

O. Roling, Prof. B. J. Ravoo
Organic Chemistry Institute and Graduate School of Chemistry
Westfälische Wilhelms-Universität Münster
Corrensstraße 40, 48149 Münster, Germany

Dr. S. Sukas, Dr. S. le Gac
BIOS Lab-on-a-Chip
University of Twente
MESA+ Institute for Nanotechnology
P.O. Box 217, 7500 AE, Enschede, Netherlands

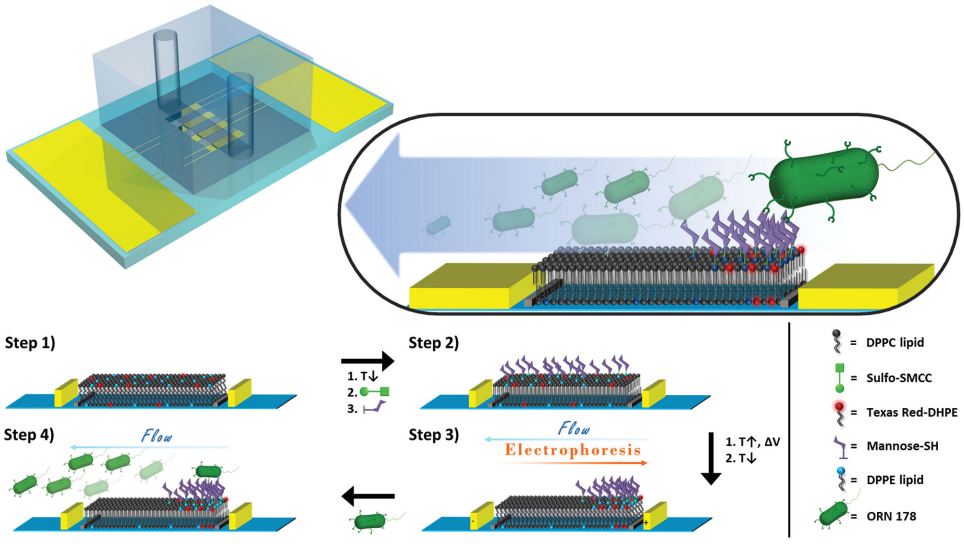

Figure 1. Microfluidic device and the steps to generate SLB-based mannose gradients for bacterial binding (see text for details). Chemical structures are given in Figure S2 (Supporting Information).

Recently, dynamic platforms have been proposed for the study of pathogen binding using supramolecular host–guest complexes.[5d,6] The surface density of a ligand can be tuned on these platforms by varying the concentration of a ligand, adding competing binding molecules in solution or by the stimulus-responsive release of ligands.[5d,6,7] Alternatively, surface-based gradient systems have been developed to probe interactions between biomolecules and surface-immobilized ligands.[8] These systems have enabled the possibility of exploring multivalent interactions over a wide range of surface densities. Despite this progress, very few gradient-based studies, i.e., microfluidic, photo- and electrochemical systems, have attempted to probe the interaction of living organisms with surfaces.[9] Here, we report the development of a supported lipid bilayer (SLB)-based gradient system in a microfluidic channel, which for the first time, allowed for the simultaneous probing of both ligand surface density and solution shear stress effects on the surface adhesion of living cells. We selected our supported lipid bilayer platform to probe the adhesion characteristics of uropathogenic *Escherichia coli* to surface-immobilized mannose via their fimbrial proteins FimH.[10] We selected our SLBs because of their nonfouling nature and ease of chemical functionalization.[11] Furthermore, we had previously reported a method to generate stable "locked-in" gradients using zwitterionic gel-state SLBs, that display negligible mobility at room temperature ($<10^{-3}$ μm^2 s^{-1}), and chemically modified them.[10a] This chip-based system will allow us here 1) to prepare continuous gradients, 2) to modify them with carbohydrate binding ligands and 3) to probe the effect of shear stress on binding of *E. coli* by varying the flow speed. Apart from bacterial binding that is dependent on the surface density of mannose, the interaction strength has been shown to increase at higher shear stresses since binding occurs through unique catch bonds.[12] As a result, the bacterium is able to mitigate the stresses from bodily fluid flow and cause infection.[13] This interesting characteristic seemed to make this an ideal pathogenic interaction system to be studied by probing it using our gradient platform.

2. Results and Discussion

To prepare mannose gradients (**Figure 1**) μSLB electrophoresis chips (Figure S1, Supporting Information) were used that have interdigitated gold electrodes (spaced 500 μm), Cr corrals (spaced 100–400 μm) and are equipped with a polydimethylsiloxane (PDMS) flow channel (5000 × 500 × 50 μm). The chips were first modified with a gel-state SLB, based on 1,2-Dipalmitoyl-sn-glycero-3-phosphocholine (DPPC) (T_m 41 °C), by means of vesicle fusion at 60 °C (Figure 1, Step 1). The high T_m of DPPC particularly provides a convenient temperature window in which no lateral mobility was observed. Included in the vesicles were 1,2-Dihexadecanoyl-sn-glycero-3-phosphoethanol-amine (DPPE) lipids, which were used for subsequent chemical modification, and fluorescent and negatively charged TR-DHPE lipids, which were used for visualization of the gradients. After cooling the chip to room temperature ($T < T_m$) the amine group of DPPE-lipids in the SLB was reacted with the heterobifunctional sulfo-SMCC crosslinker and subsequently with a thiol-functionalized mannose (mannose-SH) to yield mannose-functionalized SLBs (Figure 1, Step 2).[14] Upon heating the device above the T_m once more, μSLB electrophoresis was performed resulting in electrophoretic migration of single negatively charged mannose-modified DPPE lipids and Texas Red-1,2-dihexadecanoyl-sn-glycero-3-phosphoethanolamine (TR-DHPE) (Figure S3, Supporting Information). After 30 min of electrophoresis and continuously flowing liquid in opposite direction, the chip was rapidly cooled down to room temperature to lock the gradients in time (Figure 1, Step 3). To evaluate the binding characteristics of bacteria, the mannose gradients were incubated with *E. coli* strain ORN 178, expressing wild type FimHK514, and control strain ORN 208, expressing a mutated inactive form of FimHK514 (Figure 1, Step 4). The binding behavior of the ORN strains was further probed by monitoring the detachment of bound bacteria upon increasing the flow speed and thus shear stress (Figure 1, Step 4).

First, the modification of the SLB with mannose was validated with quartz-crystal microbalance with dissipation monitoring

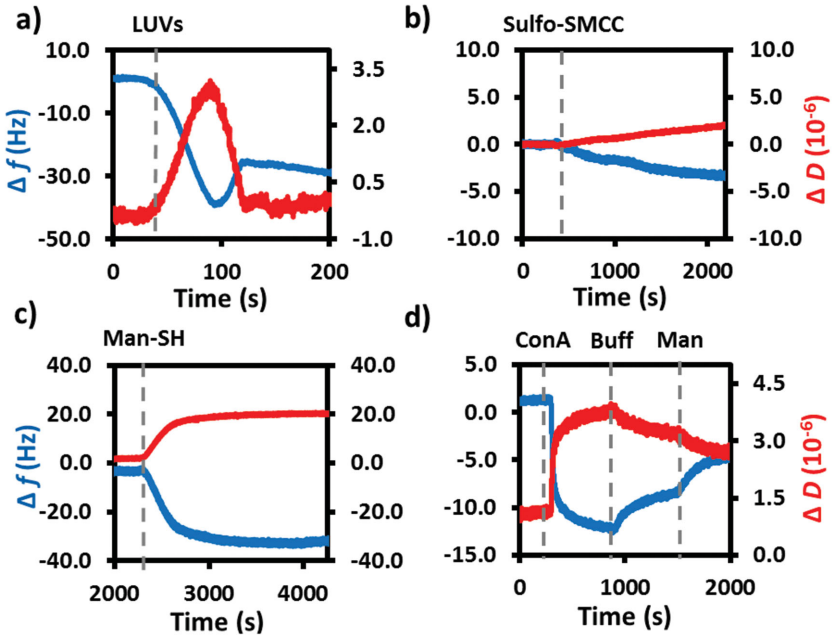

Figure 2. Evaluating mannose-modified SLB with QCM-D. a) SLB formation of an MPPC-based SLB doped with 1 mol% DPPE and 0.2 mol% TR-DHPE at 45 °C. b) Reaction of 5×10^{-3} M sulfo-SMCC and c) 1×10^{-3} M mannose-SH (Man-SH) for 30 min at r.t. d) Binding of 1×10^{-6} M ConA to mannose-modified SLB.

(QCM-D) (**Figure 2**). To this end, a borosilicate-coated QCM resonator was modified with a gel-state 1-Myristoyl-2-palmitoyl-sn-glycero-3-phosphocholine (MPPC)-based SLB (T_m 35 °C), since it yielded a more stable QCM-D response compared to DPPC. The MPPC-SLB was also doped with 0.2 mol% TR-DHPE and 1 mol% DPPE. The characteristic response of vesicle fusion leading to the formation of the SLB was observed, yielding a −25 Hz frequency change (Δf) (Figure 2a), which is in agreement with literature.[15] After cooling the chip to r.t., both the reaction of sulfo-SMCC and the subsequent conjugation of mannose-SH resulted in changes in frequency Δf and dissipation ΔD (Figure 2b,c). These changes stabilized after 30 and 50 min, respectively, indicating that the reaction was complete. A larger shift in ΔD and Δf was observed after coupling of mannose-SH, which is presumably related to a more flexible, polar and extended structure involving additional coupled water.[16]

The binding properties of the mannose-modified SLBs were assessed by flowing a 1×10^{-6} M solution of Conconavalin A (ConA) (Figure 2d). ConA is a homotetrameric lectin that is able to bind surface-immobilized mannose.[17] Binding of ConA to the mannose-modified SLB occurred within 15 min and only slowly dissociated during rinsing with buffer (Figure 2d). Upon introduction of a 10×10^{-3} M mannose solution (Man), fast dissociation of ConA from the SLB was noted. No ConA binding was observed to unmodified MPPC-SLB doped with DPPE and TR-DHPE, confirming specific interaction and the nonfouling nature of SLBs (Figure S4, Supporting Information). It must be noted that larger changes in ΔD were observed when studying gel-state MPPC SLBs. We attribute this to artifacts generated by measuring modifications on SLBs in the gel-state since liquid-state SLBs modified a priori and studied with QCM-D did not show this behavior (Figure S5, Supporting Information). The QCM-D experiments confirmed the in situ formation of DPPE-mannose and its specific interaction with ConA.

To study *E. coli* binding, mannose-SLB gradients were incubated with *E. coli* strain ORN 178 or control strain ORN 208. Specific binding of ORN 178 was observed across the device after flushing the surface to remove non-adherent cells (Figure S6, Supporting Information). The electrophoretic build-up of DPPE-mannose was deduced with TR-DHPE.[18] A control experiment where a fluorophore was conjugated to the gradients (Figure S7, Supporting Information) confirmed that the charge and density of the chemically modified DPPE lipids closely follows those of the TR-DHPE lipids. In **Figure 3**, the bacterial binding to the mannose gradient is shown for the 430 µm long corral. The adherent bacteria were given a false color and were binned. The TR-DHPE fluorescence image in Figure 3a exhibits a distinct exponential increase in fluorescence intensity along the corral. Only ORN 178 shows a clear density-dependent binding with the gradient (Figure 3b) whereas only negligible binding of control ORN 208 was noted, i.e., ≈5% compared to ORN 178 under flow conditions (Figure 3c). Control experiments performed on unmodified DPPC-based SLBs doped with DPPE and TR-DHPE revealed no interaction between the cells and the zwitterionic gel-state SLBs (Figure S8, Supporting Information), suggesting specific interaction of the FimH receptor with DPPE-mannose in the gradient. By varying the doping density of DPPE, specific regions of the binding plot for ORN 178 can be studied (Figure 3d). Figure 3d shows that a significant rise in the number of adhered bacteria by an order of magnitude occurs only in a narrow window of rising mannose density. Beyond 1 mol%, the number of adhered bacterial cells remains constant.

Based on the TR-DHPE fluorescence and DPPE-doping density, the average interligand spacing and thus mannose density could be deduced.[19] The binding data were fitted to the Hill equation and yields a K_d of 0.9×10^{-21} M, similar to the value reported by Guo and co-workers, i.e., 1.0×10^{-21} M.[20] Multivalent interaction with the gradient surface is expected since the K_d of a single FimH–mannose interaction is reported to be in the µM range.[5a] In addition, cooperative binding is suggested by a *n*-value of 4.2 (Figure S9, Supporting Information). Our experiments demonstrate that continuous SLB gradient chips can be easily employed for specificity and binding studies.[20] In addition, since our chip is equipped with a flow channel, the effect of shear stress on these binding characteristics can be simultaneously analyzed. To that end, the flow speed was varied while monitoring detachment and displacement of the bacterial cells with microscopy (**Figure 4**). To accurately describe the shear stress near the surface, a finite element simulation was performed (Figure S10, Supporting Information). In our study, shear stress values of up to ≈200 dynes cm^{-2} were evaluated. This range of values is physiologically relevant, since in vivo,

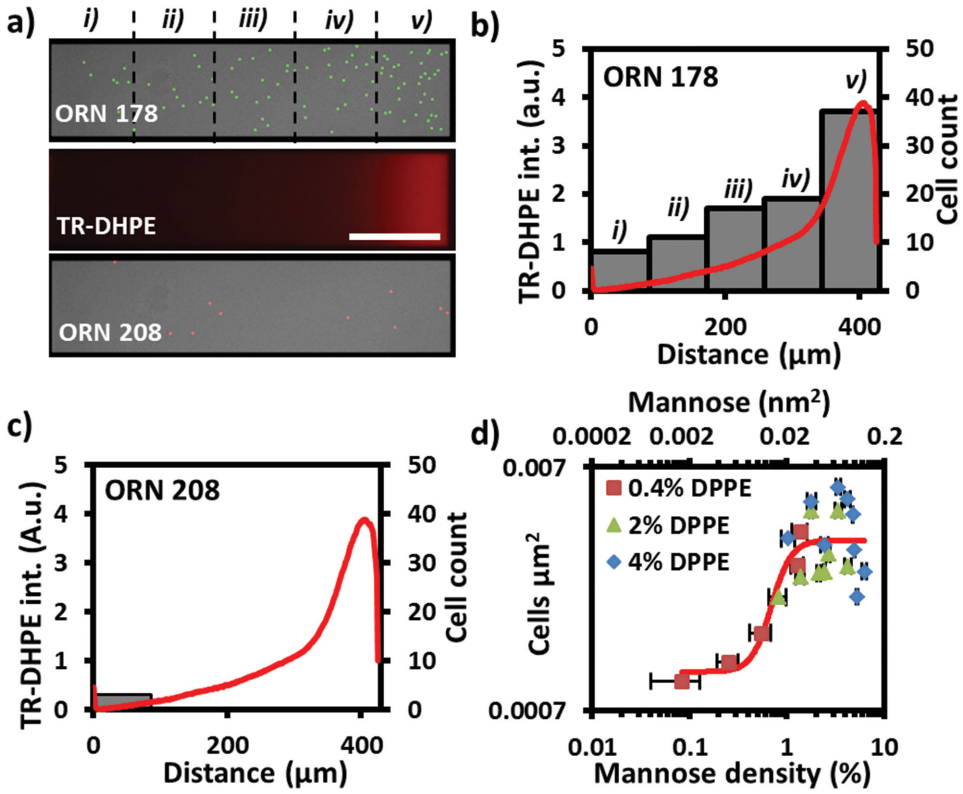

Figure 3. Bacterial adhesion to a gradient based on 0.4 mol% DPPE-mannose, 430 µm long corral. a) Bright field micrographs of ORN 178 (green) and ORN 208 (red) binding at 100 dynes cm^{-2}, scale bar 100 µm. Cell density vs. TR-DHPE fluorescence of b) ORN 178 and c) ORN 208. d) ORN 178 binding plot fitted to Hill (solid red line).

wall shear stress in human blood vessels range from a tenth, to several hundreds of dynes cm^{-2} for, e.g., veins and stenotic vessels, respectively.[21] In the region of high bacterial cell density (bin *v*), the majority (80 ± 10%) of ORN 178 cells was able to remain bound under increasing shear stress (Figure 4a). In the two regions with the lowest density of bacteria (bins *i* and *ii*) a significant reduction (28 ± 3%) of bound bacterial cells was observed upon increasing shear stress, while bins *iii* and *iv* represented an intermediate case (61 ± 3%). In the absence of flow and in the presence of cells, specific interaction of ORN 178 with the mannose surface resulted in a twice as high initial cell density compared to ORN 208 (Figure S11, Supporting Information). When these ORN 208 cells were subjected to flow with increasing shear stress, ≈95% of the initially adhered bacteria were washed away (Figure S9b, Supporting Information). In all cases, bound bacterial cells moved across the surface in the flow direction each time promptly after the flow speed was increased. In the case flow speeds were kept constant, no movement was observed. This observation is in agreement with a previous report in literature where *E. coli* movement in time was exclusively observed at very low shear stress, i.e., <10 dynes cm^{-2}, below the lowest shear stress tested in this study, i.e., 14.2 dynes cm^{-2}.[13b] The bacterial response is presumably related to stick-and-roll rolling motion of cells.[13]

However, the total displacement of adherent ORN 178 cells varied depending on their location on the gradient. In Figure 4b, the total displacement of ORN 178 was measured and compared for cells bound in bins *i* & *ii*, bins *iii* & *iv* and bin *v*. A trend of decreasing ORN 178 displacement with increasing surface density was observed, suggesting stronger surface

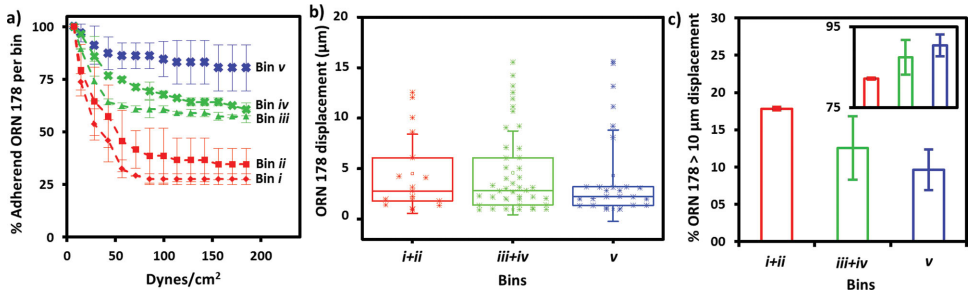

Figure 4. Effect of shear stress on ORN 178 bound to mannose-gradients. a) Percentage of adherent ORN 178 vs. shear stress in bins *i–v*. b) ORN 178 displacement in bins *i-ii, iii-iv,* and *v* and c) the % ORN 178 cells that moved >10 µm (inset <10 µm). Blue bin *v*, green bins *iii+iv* and red, bins *i+ii*.

interaction of ORN 178 in bin *v*. This is confirmed by grouping ORN 178 cells that either moved more than 10 µm or less than 10 µm in bins *i* & *ii*, bins *iii* & *iv* and bin *v* (Figure 4c). The amount of cells that moved less than 10 µm was significantly higher for the region of the highest density of mannose (bin *v*) supportive of stronger surface interaction of the bacteria in this region. While the amount of cells that moved a distance of more than 10 µm decreased with increasing mannose surface density, highlighting the effect of mannose density on total bacterial displacement in flow conditions. Interesting to note is the nonlinear behavior shown in Figure 4a, most evident in bins *iii* & *iv*. Here, stabilization of the amount of adhered cells with increasing shear stresses seems to suggest an increased in binding strength between surface-bound mannose and the bacteria. Since the density of mannose remains the same, the increase in binding strength may presumably be related to so-called catch bonds, force-induced increase of the lifetime of individual receptor–ligand interactions.[13b]

3. Conclusion

In conclusion, the device was successfully prepared and characterized. Continuous gradients of model ligand mannose were prepared, characterized, and used to evaluate the binding of *E. coli* strain ORN 178. Using this model system, we demonstrated that FimH binding to the continuous locked-in mannose gradients was specific and shows selective binding above a threshold density of mannose. Moreover, the effect of shear stress on the binding and total displacement of ORN 178 cells was investigated. A dependency was found between increasing mannose density, increasing cell adherence and decrease of total cell displacement. Bacteria bound to regions of highest mannose density on the SLB gradient were most prone to retain their cell–surface interactions. Our microfluidic-SLB platform is useful for engaging with a semi-high-throughput analysis of pathogen–lectin interaction by easily varying the ligand density over a wide range and probing the binding under physiologically relevant shear conditions. Our gradient chip easily probes the threshold binding in pathogen–lectin interactions and makes the study of catch bonds more accessible.

4. Experimental Section

Experimental procedures and sample preparation, Figures S1–S9 can be retrieved from the Supporting Information.

Supporting Information

Supporting Information is available from the Wiley Online Library or from the author.

Acknowledgements

J.v.W. and S.S. contributed equally to this work. NanoNextNL is acknowledged for funding through the program 3B (Nanofluidics for Lab-on-a-chip) to S.L.G. and through 6C (Nano-bio interfaces and devices) to M.K. and P.J. The European Research Council is acknowledged for a Starting Grant (Sumoman 259183) to P.J. The Chemical Council of the Dutch Science Foundation is acknowledged through a VIDI grant (Molecularly engineering cell-material interfaces723.012.106) to P.J. O.R. acknowledges a fellowship of the Graduate School of Chemistry in Münster. The Bionanlab facilities of the MESA+ Institute for Nanotechnology are highly appreciated.

Received: January 21, 2016
Revised: February 6, 2016
Published online: March 7, 2016

[1] a) L. L. Kiessling, J. E. Gestwicki, L. E. Strong, *Curr. Opin. Chem. Biol.* **2000**, *4*, 696; b) T. J. C. Harris, U. Tepass, *Nat. Rev. Mol. Cell Biol.* **2010**, *11*, 502.

[2] a) C. Ottone, B. Krusche, A. Whitby, M. Clements, G. Quadrato, M. E. Pitulescu, R. H. Adams, S. Parrinello, *Nat. Cell Biol.* **2014**, *16*, 1045; b) F. Peglion, F. Llense, S. Etienne-Manneville, *Nat. Cell Biol.* **2014**, *16*, 639.

[3] a) M. Bischoff, R. Schnabel, *Dev. Biol.* **2006**, *294*, 432; b) S. Etienne-Manneville, *Oncogene* **2008**, *27*, 6970; c) A.-I. Zaromytidou, *Nat. Cell Biol.* **2012**, *14*, 990.

[4] a) M. Mrksich, *Chem. Soc. Rev.* **2000**, *29*, 267; b) P. H. Liang, C. Y. Wu, W. A. Greenberg, C. H. Wong, *Curr. Opin. Chem. Biol.* **2008**, *12*, 86.

[5] a) J. Bouckaert, J. Mackenzie, J. L. de Paz, B. Chipwaza, D. Choudhury, A. Zavialov, K. Mannerstedt, J. Anderson, D. Pierard, L. Wyns, P. H. Seeberger, S. Oscarson, H. De Greve, S. D. Knight, *Mol. Microbiol.* **2006**, *61*, 1556; b) P. H. Liang, S. K. Wang, C. H. Wong, *J. Am. Chem. Soc.* **2007**, *129*, 11177; c) R. J. Pieters, *Org. Biomol. Chem.* **2009**, *7*, 2013; d) J. Voskuhl, S. Sankaran, P. Jonkheijm, *Chem. Commun.* **2014**, *50*, 15144.

[6] S. Sankaran, J. van Weerd, J. Voskuhl, M. Karperien, P. Jonkheijm, *Small* **2015**, *11*, 6187.

[7] Z. Qi, P. Bharate, C.-H. Lai, B. Ziem, C. Böttcher, A. Schulz, F. Beckert, B. Hatting, R. Mülhaupt, P. H. Seeberger, R. Haag, *Nano Lett.* **2015**, *15*, 6051.

[8] a) J. D. Wu, Z. W. Mao, H. P. Tan, L. L. Han, T. C. Ren, C. Y. Gao, *Interface Focus* **2012**, *2*, 337; b) S. O. Krabbenborg, J. Huskens, *Angew. Chem., Int. Ed.* **2014**, *53*, 9152.

[9] a) J. Lee, I. Choi, W. S. Yeo, *Chem. Eur. J.* **2013**, *19*, 5609; b) J. Almodovar, T. Crouzier, S. Selimovic, T. Boudou, A. Khademhosseini, C. Picart, *Lab Chip* **2013**, *13*, 1562; c) E. J. Lee, E. W. L. Chan, W. Luo, M. N. Yousaf, *RSC Adv.* **2014**, *4*, 31581.

[10] a) S. O. Krabbenborg, J. van Weerd, M. Karperien, P. Jonkheijm, J. Huskens, *ChemPhysChem* **2014**, *15*, 3460; b) J. v. Weerd, *PhD thesis, University of Twente* January, **2015**.

[11] a) L. K. Tamm, H. M. Mcconnell, *Biophys. J.* **1985**, *47*, 105; b) E. Sackmann, *Science* **1996**, *271*, 43; c) K. Salaita, P. M. Nair, R. S. Petit, R. M. Neve, D. Das, J. W. Gray, J. T. Groves, *Science* **2010**, *327*, 1380; d) P. M. Nair, K. Salaita, R. S. Petit, J. T. Groves, *Nat. Protoc.* **2011**, *6*, 523; e) V. Malinova, M. Nallani, W. P. Meier, E. K. Sinner, *FEBS Lett.* **2012**, *586*, 2146; f) S. M. Schiller, in *Handbook of Biofunctional Surfaces*, (Ed: W. Knoll), Pan Stanford Publishing Pte. Ltd., Singapore **2013**, Ch. *18*.

[12] S. Hertig, V. Vogel, *Curr. Biol.* **2012**, *22*, R823.

[13] a) W. E. Thomas, E. Trintchina, M. Forero, V. Vogel, E. V. Sokurenko, *Cell* **2002**, *109*, 913; b) L. M. Nilsson, W. E. Thomas, E. V. Sokurenko, V. Vogel, *Appl. Environ. Microbiol.* **2006**, *72*, 3005.

[14] C. E. Ashley, E. C. Carnes, G. K. Phillips, D. Padilla, P. N. Durfee, P. A. Brown, T. N. Hanna, J. Liu, B. Phillips, M. B. Carter, N. J. Carroll, X. Jiang, D. R. Dunphy, C. L. Willman, D. N. Petsev,

D. G. Evans, A. N. Parikh, B. Chackerian, W. Wharton, D. S. Peabody, C. J. Brinker, *Nat. Mater.* **2011**, *10*, 389.
[15] R. P. Richter, A. R. Brisson, *Biophys. J.* **2005**, *88*, 3422.
[16] F. Hook, B. Kasemo, T. Nylander, C. Fant, K. Sott, H. Elwing, *Anal. Chem.* **2001**, *73*, 5796.
[17] D. Dechtrirat, N. Gajovic-Eichelmann, F. Wojcik, L. Hartmann, F. F. Bier, F. W. Scheller, *Biosens. Bioelectron.* **2014**, *58*, 1.
[18] J. T. Groves, S. G. Boxer, H. M. McConnel, *Proc. Natl. Acad. Sci. USA* **1997**, *94*, 13390.
[19] A. Korner, C. Deichmann, F. F. Rossetti, A. Kohler, O. V. Konovalov, D. Wedlich, M. Tanaka, *PLoS One* **2013**, *8*, e54749.
[20] X. Y. Zhu, B. Holtz, Y. Wang, L.-X. Wang, P. E. Orndorff, A. Guo, *J. Am. Chem. Soc.* **2009**, *131*, 13646.
[21] D. L. Brown, *Cardiovascular Plaque Rupture*, Marcel Dekker, New York **2002**.